Journal of Statistical Physics, Vol. 89, Nos. 3/4, 1997

Hybrid Neural Nets with Poisson and Gaussian Connectivities

E. Fournou,[1,2] P. Argyrakis,[1] B. Kargas,[3] and P. A. Anninos[4]

Received April 10, 1995; final March 25, 1997

The dynamic behavior of neural nets with different patterns of interneuronal synaptic connectivity is investigated. Our method is based on probabilistic neural nets for the net structure and dynamics. Each net is divided into several different subsystems, which are characterized by different distribution laws for the number of connections that the neurons make. We start from the binomial distribution, which, under appropriate conditions, reduces to the Poisson and Gaussian distributions. The overall net now acquires a hybrid character. The expression for the neural activity is generalized to include this effect, and new expressions are derived, based on the isolated single-net equations. The dynamics of nets with sustained external inputs is also studied. The results obtained by this approach also show multiple stability and multiple hysteresis effects, as in the case of single nets. The differences between pure Poisson, Gaussian, and hybrid nets are explained in terms of the structural properties of the model. As expected, the hybrid case falls in between the two other distributions. Finally, we performed Monte Carlo computer calculations for the hybrid nets. For the range of parameters examined we find very good agreement with the developed formalism.

KEY WORDS: Neural net; neural modeling; chemical markers; Poisson distribution of connectivities; Gaussian distribution of connectivities.

[1] Department of Physics, University of Thessaloniki, 54006 Thessaloniki, Greece.
[2] Permanent address: Department of Applied Sciences, Technological Education Institution (TEI) of Thessaloniki, 57400 Sindos, Greece.
[3] Department of Applied Sciences, Technological Education Institution (TEI) of Thessaloniki, 57400 Sindos, Greece.
[4] Department of Medical Physics, University of Thraki, 68100 Alexandroupolis, Greece.

0022-4715/97/1100-0847$12.50/0

1. INTRODUCTION

Over the past three decades neural nets have been a subject of intensive studies from several points of view. An area with considerable importance is that of biological nets, i.e., models of nets that try to imitate the human or other living brain structure and functions in an effort to understand such vital processes as learning, memory, understanding, feeling, etc. Widely used models (not an exhaustive list) include the early pioneer work of McCulloch and Pitts of assemblies of neurons as logical decision elements,[1] the mathematical formalism of Caianiello of the "neuronic equation,"[2] and the probabilistic neural structures[3–6] that monitor the net activity, i.e., the fraction of neurons that become active per unit time. All these models have been somewhat successful in the improvement of our understanding of the above mentioned functions. In these models a network is made of a large number of neurons, which are interconnected according to some rules. As each unit has several connections, and there is a large number of units, it is quickly realized that the number of connections grows very fast, making the task of calculations quite difficult. But it should be realized that it is exactly this complicated connectivity structure that produces the collective properties that neural nets possess.

The effect of the structure on the function and on the dynamic behavior in neural nets has been also a subject of considerable interest in recent years. In the so called probabilistic nets we have an assembly of a large number of neurons, randomly positioned in space, that have only partial connectivity, i.e., each neuron is connected to only a very small fraction of the total number of neurons in the system, randomly chosen. The accepting neurons are also chosen at random, so that one ends up with a complex looking, albeit fixed pattern, but somewhat difficult to draw. More details for typical parameter values are given later in the simulation section. The principal idea is that this connectivity is given by the binomial distribution. Since here we deal with a very large number of units (neurons), the binomial distribution is customarily reduced to the Poisson distribution. In early work, quite simple probabilistic isolated neural nets were investigated with Poisson or Gaussian distribution of interneuronal connectivity.[7] The main conclusion of the past work was that when a neuron was connected to a relatively small number of units, only a Poisson distribution law was appropriate, while if it were connected to a large number of units, also a Gaussian law was a fairly good approximation.

More complex characteristics were later included with the concept of chemical markers.[6, 8, 9] A neural net with chemical markers is divided in several subpopulations, each one characterized by its own chemical marker. The idea of a different marker for each subpopulation of the net is that,

even though there are structural connections between any neurons of the net (say, at random), only these connections are active (i.e., carry signal) for which the initial and final neurons belong to the same marker. If they belong to different markers then the connection exists but it is inactive. The implication is that a neuron makes active synaptic connections only with those neurons in the net which carry markers with the highest chemical affinity to its own. This idea is according to the theory of neural specificity.[10-12]

The average number of synaptic connections turns out to be the main structural parameter of significant interest for the dynamic behavior of the model, and therefore, the distribution law for the connectivities plays an important role. The behavior of a net can be monitored through its activity (a_n), which is defined as the fraction of neurons out of the total number ($0 \leqslant a_n \leqslant 1$) that become active in one unit of time. Initially the net at time $t = 0$ is at rest, and carries no signal. At a given time an initial stimulus is supplied that activates a small fraction of neurons. This small fraction is a_n. Subsequently, this activity is propagated throughout the net (for details see the model description), in such a way that a_n becomes time dependent. It is of interest to follow the time course of such a net. In the past,[5] depending on the progress of the initial activity, it was found that a net may belong to one of three classes: A (if it sustains a finite non-zero activity for any input over the course of time), B (if it sustains an activity only for inputs above a certain threshold), or C (if it can never sustain an activity, regardless of the initial input). In the present study we also use these criteria to investigate how a net is affected by the interplay of the distribution laws of the neuron connectivities.

The theoretical basis in the probabilistic nets is to derive expressions for the probability that a neuron is active (i.e., firing). This is done through basic principles starting with the binomial distribution, as one tries to attribute some specific properties to a fraction of units out of the total population. The mathematical formalism is quite involved, but it is straightforward.[5] We also propose and use Computer simulations of the dynamics described here, using typical values of the parameters that make up this problem. Specifically, we use a Monte Carlo technique that generates nets by making specific connections between a large number of neurons. These connections stay frozen for the entire duration of the calculation. Then, the net is divided in several markers which also stay frozen in the entire calculation. The net activity is calculated numerically. By this method we try to imitate all the conditions and dynamics described in the formalism, and it is interesting to find out if the results from the two techniques agree for the range of parameters studied.

In the present work we investigate the possibility that different subsystems of a neural net have different connectivity patterns, given by

different distribution laws. Some may be Poissonian, and some Gaussian. The different connectivities are assigned to sections with different markers. Thus, each marker is characterized by either one of these distributions according to the magnitude of the connections that its neurons make, as described above. We consider nets with various differences in their structural parameters among their subsystems, such as nets with some subsystems having large number of synaptic connections and some subsystems having small number of connections. Isolated as well as non-isolated neural nets are used. In Section 2 we describe the general assumptions of the model, as previously used, and include a glossary of the symbols used. In Section 3 we present the development of the formalism that incorporates the two different distributions. In Section 4 we present details of the simulation method used. In Section 5 we give some numerical examples and results of the formalism developed here, and finally in Section 6 the conclusions of this work. In the appendix we give details of the proof of Eq. (17), which gives the slope of the curve a_{n+1} vs a_n as $a_n \to 0$, in the general case of isolated hybrid neural nets with chemical markers.

2. THE NEURAL MODEL

2.1. List of Symbols

The subscript j is a marker label and indicates the properties of a subpopulation in the network characterized by the jth marker.

Structural parameters of the neural net

A Total number of neurons in the net
N Number of markers (subsystems)
m_j Fraction of neurons carrying the jth marker in the net
h_j Fraction of inhibitory neurons
h_o Fraction of external inhibitory neurons (fibers)
μ_j^+ The average number of neurons receiving excitatory postsynaptic potentials (EPSPs) from one excitatory neuron
μ_j^- The average number of neurons receiving inhibitory postsynaptic potentials (IPSPs) from one inhibitory neuron
$\mu_o^\pm$ The average number of neurons in each subsystem with which an external excitatory/inhibitory neuron (fiber) makes its synaptic contacts (receiving external excitatory/inhibitory PSPs from one external fiber)
K_j^+ The size of PSP produced by an excitatory neuron of the net
K_j^- The size of PSP produced by an inhibitory neuron of the net

$K_o^{\pm}$ The average PSP produced by external excitatory/inhibitory fibers in the net

ϑ_j Firing threshold of neurons of the jth marker

Dynamical parameters

n An integer giving the number of elapsed synaptic delays

τ Synaptic delay

r Refractoriness

a_n The activity, i.e., the fractional number of active neurons in the net at time $t = n\tau$

σ The fractional number of external active fibers (carrying action potentials at a particular instant)

2.2. Description of the Model

Neural nets are assumed to be constructed of discrete sets of randomly interconnected neurons of similar structure and function. The neural connections are set up by means of chemical markers carried by the individual cells. Thus, the neural population of the net is treated as a set of subpopulations of neurons, each of them characterized by a specific chemical marker. At each subsystem we attribute the appropriate, Poissonian or Gaussian, distribution law for their connectivities.

The elementary unit, the neuron, is a bistable element. It can be either in a resting or in an active (firing) state. The transition from the resting to the firing state of the neuron occurs when the sum of *postsynaptic potentials* (PSPs) arriving at the cell exceeds the firing threshold ϑ of the neuron. PSPs may be either excitatory (EPSPs) or inhibitory (IPSPs), shifting the membrane potential closer to or further away from ϑ, respectively. Each neuron at some instance may carry an electrical potential of a few millivolts, which it passes on to the neurons that it is connected to.

In this model, a net with N markers is assumed to be constructed of A formal neurons. A fraction h $(0 < h < 1)$ of them are inhibitory with all of their axon branches generating IPSPs, while the rest are excitatory with all of their axon branches generating EPSPs. Each neuron receives, on the average, μ^+ EPSPs and μ^- IPSPs. The size of the PSP produced by an excitatory (inhibitory) unit is $K^+(K^-)$. In addition to the net constructed, we assume that there also exists some other external net, which is connected to it by a cable of afferent fibers. The regular net is considered to receive sustained inputs from this external net. This external net has A_o neurons with the same structure as the regular net. A fraction h_o $(0 < h_o < 1)$ of them are inhibitory. A parameter σ $(0 < \sigma < 1)$ is used to describe the external sustained input, and denotes the fraction of external

active fibers, carrying action potentials at a particular instant from outside. With $\mu_o^+(\mu_o^-)$ we denote the average number of neurons in each subsystem with which an external excitatory (inhibitory) neuron makes its synaptic connections in the regular net, while $K_o^+(K_o^-)$ are the corresponding strengths of the synaptic coupling coefficients. Other than the parameter values of the external net we are not interested in the details of its structure and functions, except that it provides an input of additional signals to our normal net.

The dynamics of the net is monitored by inputting a certain initial signal at time $t=0$ to some units in the net, and observing its propagation throughout the net and the results it produces. The neurons are also characterized by the absolute refractory period and the synaptic delay τ. If a neuron fires at time t, it produces the appropriate PSPs after a fixed time interval τ, the *synaptic delay*. PSPs arriving at a neuron are summed instantly, and if this sum is greater or equal to ϑ, then the neuron will fire immediately, otherwise, it will be idle. PSPs (if below ϑ) will persist with or without decrement for a period of time called the *summation time*, which is assumed to be less than the synaptic delay. Firing is momentary and causes the neuron to be insensitive to further stimulation for a time interval called the (*absolute*) *refractory period.* Here, it is assumed that the refractory period is greater than the synaptic delay, but less than twice the synaptic delay. A parameter r for the refractory period may be used, taking, in general, any integer value. For our purposes r was given the value $r=1$ when refractoriness is assumed, or $r=0$ otherwise. From these assumptions it follows that if a number of neurons fire simultaneously at time t, then all neural activity resulting from this initial activity will be restricted to times $t+\tau, t+2\tau,...$

3. DYNAMICS OF HYBRID NEURAL NETS

Consider a net of A neurons and N markers. Due to the presence of markers the net is divided to N subpopulations. If $m_1, m_2,..., m_N$ are the fractions of neurons out of the total, corresponding to each subpopulation, then $m_1+m_2+\cdots+m_N=1$. Such a net may be isolated or non-isolated. In the later case the net is attached to a cable of afferent fibers receiving through it sustained inputs from another net of A_o neurons with the same structure, a fraction h_o $(0<h_o<1)$ of which are inhibitory. A fraction σ are active fibers, i.e., they carry action potentials at a particular instant from outside. It is assumed that σ is constant or slowly changing, and the number σA_o of active fibers is chosen randomly at each time interval τ. The average number of neurons in each subsystem with which an external excitatory (inhibitory) neuron makes its synaptic connections in the net is

denoted by $\mu_o^+(\mu_o^-)$, and the corresponding strength of the synaptic coupling coefficient by $K_o^+(K_o^-)$.

The dynamic variable of interest is as usual the neural activity a_n, which is the fraction of neurons in the net (out of the total) that are active at time $t=n\tau$. This quantity is a scalar and does not specify which particular neurons are firing in the net. The quantity a_n at time $t=n\tau$ depends exclusively on the firing record of the net at time $t=(n-1)\tau$, i.e., the previous time unit. Therefore, the dynamics of the net is a Markov process. The activity, a_{n+1}, will depend on whether there is refractoriness or not ($r=0$ or $r=1$).

For the case of no refractoriness in any subsystem ($r=0$ for all subsystems), the number of neurons in the jth marker available for triggering at $t=n\tau$ is Am_j. If P_j is the probability of triggering a particular neuron of the jth marker, then Am_jP_j will be the number of firing neurons of this marker at the next time step $t=(n+1)\tau$. Thus the expression for the neural activity a_{n+1} is:

$$a_{n+1}=\sum_{j=1}^{N} m_jP_j \tag{1}$$

For the case of refractoriness ($r=1$) the neurons which are active at $t=n\tau$ will be inactive at the next time step $t=(n+1)\tau$, so there will be exactly $(1-a_n)\,Am_j$ neurons in the jth marker that will not be in refractory state at this time step. Thus, the activity a_{n+1} is now:

$$a_{n+1}=(1-a_n)\sum_{j=1}^{N} m_jP_j \tag{2}$$

Let us look in detail at the nature of P_j, the probability of triggering a particular neuron of the jth marker. P_j is obtained by adding the probabilities of all combinations of excitatory and inhibitory inputs to that neuron, which give a total PSP exceeding the threshold, ϑ, at $t=(n+1)\tau$. In the jth marker a fraction $(1-h_j)$ of neurons out of Am_j are excitatory, and each of them has, on the average, μ_j^+ afferent connections. If a_n is the fraction of active neurons in the net at $t=n\tau$, then a number of $Aa_n\mu_j^+(1-h_j)\,m_j$ EPSP's will appear in the jth marker, at $t=(n+1)\tau$. Since the connections are random, each of these has a probability $1/A$ of landing on a particular neuron, and the average number of EPSP's per neuron will be $a_n\mu_j^+(1-h_j)\,m_j$. Thus, the probability $P_{L,j}$ that a neuron receives L EPSP's is given by the binomial distribution:

$$P_{L,j}=\binom{Aa_n\mu_j^+(1-h_j)\,m_j}{L}\left(\frac{1}{A}\right)^L\left(1-\frac{1}{A}\right)^{Aa_n\mu_j^+(1-h_j)\,m_j-L} \tag{3}$$

which can be approximated by the Poisson distribution:

$$P_{L,j} = [a_n \mu_j^+ (1 - h_j) m_j]^L \exp[-a_n \mu_j^+ (1 - h_j) m_j]/L! \tag{4}$$

because $(1/A) \ll 1$ and $A a_n \mu_j^+ (1 - h_j) m_j \gg 1$.

Similar expressions are obtained for the probabilities $Q_{I,j}$ and $R_{M,j}$ that a neuron receives I IPSP's and M external PSP's, respectively. These quantities are given below.

Since the purpose of this paper is to investigate further the effect of different distributions laws[7] and different combinations of these laws, we have to generalize Eqs. (1) or (2). In the present model we further assume that $N_1 (N_1 < N)$ subpopulations are characterized by low interneuronal connectivity, i.e., the parameter $\mu^+ (\mu^-)$ is relatively small so that the Poisson approximation is valid, whereas the remaining $N_2 (N_2 = N - N_1)$ are characterized by high connectivity, i.e., the parameter $\mu^+ (\mu^-)$ is large and the Gaussian approximation is valid. For a net with strong differentiation in the interneuronal connectivity among its subsystems, the a_{n+1} quantity can be expressed both by Poisson and Gaussian terms. In this case Eq. (2) takes the following form

$$a_{n+1} = (1 - a_n) \left(\sum_{j=1}^{N_1} m_j P_{Pj} + \sum_{j=N_1+1}^{N} m_j P_{Gj} \right), \tag{5}$$

where we now have two sums instead of one, the first describing the Poisson contribution, and the second the Gaussian contribution.

In Eq. (5) $P_{Pj} = P_{Pj}(a_n, m_j, \sigma, \vartheta_j)$ is the probability that a neuron of the jth marker receives a total PSP which exceeds its threshold ϑ_j, for the Poisson approximation, and it is given by[6]

$$P_{Pj}(a_n, m_j, \sigma, \vartheta_j) = \sum_{M=0}^{M\max,j} \sum_{I=0}^{I\max,j} \left(1 - \sum_{L=0}^{\eta_j' - 1} P_{L,j} \right) Q_{I,j} R_{M,j} \tag{6}$$

where $P_{L,j}$ is given by Eq. (4) and:

$$Q_{I,j} = (a_n \mu_j^- h_j m_j)^I \exp(-a_n \mu_j^- h_j m_j)/I! \tag{7}$$

$$R_{M,j} = (\sigma \mu_o^{\pm} m_j)^M \exp(-\sigma \mu_o^{\pm} m_j)/M! \tag{8}$$

$$I_{\max,j} = A a_n \mu_j^- h_j m_j \tag{9}$$

$$M_{\max,j} = A_o \sigma \mu_o^{\pm} m_j \tag{10}$$

and

$$\eta_j' = u[(\vartheta_j + I K_j^- \mp M K_o^{\pm})/K_j^+] \tag{11}$$

The function u[x] is defined as the smallest integer which is equal to or greater than x.

If the average number of active inputs per neuron becomes sufficiently large, as in the N_2 markers, the number of PSPs per neuron will follow a Gaussian distribution. In this case, the quantity $P_{Gj} = P_{Gj}(a_n, m_j, \sigma, \vartheta_j)$ is calculated in analogy to our previous studies (Fournou, Argyrakis and Anninos, 1993). If l_j and i_j are the numbers of EPSPs and IPSPs, respectively, that are inputs to a given neuron of the jth marker emanating from the net itself, and if l'_j, i'_j are the numbers of External EPSPs and IPSPs, respectively, that are inputs to this neuron emanating from the axons, then the total PSP input to a given neuron of the jth marker at time $t = (n+1)\tau$ will be given by

$$e_{j,n+1} = l_j K^+ + i_j K^- + l'_j K_o^+ + i'_j K_o^- \tag{12}$$

If all the quantities l_j, i_j, l'_j and i'_j are sufficiently large, their distributions may be approximated by normal distributions about their average values $\bar{l}_j = a_n \mu_j^+ (1-h_j)\, m_j$, $\bar{i}_j = a_n \mu_j^- h_j m_j$, $\bar{l}'_j = (A_o/A)\, \sigma \mu_o^+ (1-h_o)\, m_j$ and $\bar{i}'_j = (A_o/A)\, \sigma \mu_o^- h_o m_j$. Thus, the distribution of $e_{j,n+1}$ will be also a Gaussian distribution with average value:

$$\begin{aligned} \bar{e}_{j,n+1} = {} & a_n m_j [\mu_j^+ (1-h_j)\, K^+ + \mu_j^- h_j K^-] \\ & + \frac{A_o}{A}\, \sigma m_j [\mu_o^+ (1-h_o)\, K_o^+ + \mu_o^- h_o K_o^-] \end{aligned} \tag{13}$$

and variance:

$$\begin{aligned} \delta_{j,n+1}^2 = {} & a_n m_j [\mu_j^+ (1-h_j)(K^+)^2 + \mu_j^- h_j (K^-)^2] \\ & + \frac{A_o}{A}\, \sigma m_j [\mu_o^+ (1-h_o)(K_o^+)^2 + \mu_o^- h_o (K_o^-)^2] \end{aligned} \tag{14}$$

since the probabilities of l_j, i_j, l'_j and i'_j are independent of each other.

The probability $P_{Gj} = P_{Gj}(a_n, m_j, \sigma, \vartheta_j)$ that a neuron of the jth marker receives a total PSP which exceeds its threshold ϑ_j is now

$$P_{Gj}(a_n, m_j, \sigma, \vartheta_j) = \frac{1}{\sqrt{2\pi}} \int_{x_{j,n+1}}^{\infty} e^{-x^2/2}\, dx \tag{15}$$

where

$$x_{j,n+1} = \frac{\vartheta_j - \bar{e}_{j,n+1}}{\delta_{j,n+1}} \tag{16}$$

We can use the above equations for the case of isolated neural nets if we put $\sigma = 0$, which would reduce them to those derived in previous work.[8]

The slope at the point $a_n = 0$ of Eq. (5) is easily taken by combining the relevant results with Poisson and Gaussian approximations (for the details see the appendix). Thus, we have:

$$\left.\frac{\partial a_{n+1}}{\partial a_n}\right|_{a_n=0} = \begin{cases} \sum_{j=1}^{N_1} m_j^2 \mu_j^+ (1-h_j) & (\eta_j = 1) \\ 0 & (\eta_j \geqslant 2) \end{cases} \tag{17}$$

where the parameter η_j is defined as the minimum number of EPSPs necessary to trigger a neuron of the jth marker in absence of inhibitory inputs, and it is given by $\eta_j = u[\vartheta_j / K_j^+]$. In this equation, as expected, there is no contribution of the N_2 Gaussian subpopulations to the slope of a_{n+1} at $a_n = 0$, since the Gaussian distribution slope is always zero at the origin. This results in the absence of class A from the Gaussian nets.[8] However, Eq. (17) suggests that in neural nets with hybrid interneuronal connectivity, due to the Poisson components, all three classes, A, B and C will exist in their classification.

4. SIMULATION MODEL

We developed a simulation algorithm to calculate the quantities of Eq. (5) directly. Typically, a net contains A = 1000 neurons, which are subdivided into N markers, usually N = 2, 3, or 4. By use of a random number generator we determine the connectivities that are to be realized, following the prevailing law, i.e., Poisson, Gaussian, or hybrid. Thus, the appropriate neuronal connectivity matrix $\{k_{ij}\}$ is first constructed. Each element k_{ij} denotes the synaptic strength of the connection from j to i neuron (coupling coefficient). This may take either positive or negative values depending on the type of the synaptic neuron (excitatory or inhibitory, respectively). The macroscopic parameters K^+, K^-, μ^+, μ^- are considered to vary randomly between a maximum and a minimum value, and their specific values are again determined by use of a random number generator. Thus, for the same structural parameters, we can obtain a different microscopical structure of the net, by using a different seed for the random number generator. Once constructed a net remains "frozen" regarding its connections for the entire duration of calculations.

The net is activated by specifying randomly a set of neurons which are taken to be active at time $t = 0$. One synaptic delay later all neurons linked to them will receive the appropriate inputs. The inputs arriving at a neuron

are summed instantly, and if the sum exceeds the neuron threshold then the neuron will fire. At the next time step all active neurons are specified. The firing neurons for the time step $t = n\tau$ define the state vector $\mathbf{a}_n$. Refractoriness of neurons is taken into account by imposing that a neuron that has fired at some moment $t = n\tau$ cannot fire at $t = (n+1)\tau$. The dynamics of the net is followed for n time units, by monitoring the net activity, which is the fraction of active neurons out of the total number of neurons.

Eventually, for a set of parameters we perform typically 100 different realizations, and average the resulting data. The reason of this averaging is that we found that a single run contains inherently some statistical fluctuations, which are thus averaged out. Each realization is performed on a new microstate of the system, prepared with the same parameter values, but different initial random number generator seed. Thus, these results are to be interpreted as Monte Carlo simulation results.

5. RESULTS AND EXAMPLES

In this section we present solutions (representations) of the above equations and some numerical examples that exemplify the combinations of the two distributions. The basic equation is Eq. (5) with the corresponding expressions for the Poisson (P_{Pj}) and Gaussian (P_{Gj}) terms. We first examine the case of isolated nets with refractoriness ($r = 1$), and $\eta = 1$ (see Eq. (17)), in order to see the effect of one subsystem with Poisson characteristics on the configuration of the class of a net, since class A may exist only in Poisson nets. We used nets with four markers, $m_a = 0.4$, $m_b = 0.3$, $m_c = 0.2$ and $m_d = 0.1$, with $\eta = 1$, $h = 0$ and $\mu^+ = 20$, which is relatively small (not adequate) for the Gaussian approximation, and $\mu^+ = 200$, which is relatively large. For each one of these two values of the

Table 1. The Values of $m_j^2\mu^+(1-h)$ and the Slope at $a_n = 0$ of the Activity for Each Subpopulation of Fig. 1 with Four Markers and $\mu^+ = 20$, $h = 0$, $\eta = 1$[a]

			Slope at $a_n = 0$					
	m_j	$m_j^2\mu^+(1-h)$	P	P_aG	P_bG	P_cG	P_dG	G
a	0.4	3.2	3.2	3.2	0	0	0	0
b	0.3	1.8	1.8	0	1.8	0	0	0
c	0.2	0.8	0.8	0	0	0.8	0	0
d	0.1	0.2	0.2	0	0	0	0.2	0
		Net	6	3.2	1.8	0.8	0.2	0
		Class	A	A	A	B	B	B

[a] The slope of the curve of total activity and the class of the corresponding net.

Table 2. The Values of $m_j^2\mu^+(1-h)$ and the Slope at $a_n=0$ of the Activity for Each Subpopulation of Fig. 2 with Four Markers and $\mu^+=200$, $h=0$, $\eta=1$[a]

			Slope at $a_n=0$					
	m_j	$m_j^2\mu^+(1-h)$	P	$P_\alpha G$	$P_b G$	$P_c G$	$P_d G$	G
a	0.4	32	32	32	0	0	0	0
b	0.3	18	18	0	18	0	0	0
c	0.2	8	8	0	0	8	0	0
d	0.1	2	2	0	0	0	2	0
		Net	6	32	18	8	2	0
		Class	A	A	A	A	A	B

[a] The slope of the curve of total activity and the class of the corresponding net.

parameter μ^+, we obtained plots of a_{n+1} vs a_n for the following six cases of nets: Net P, with all its subpopulations having Poisson characteristics; nets $P_\alpha G$, $P_b G$, $P_c G$ and $P_d G$ with only one subpopulation (indicated by the corresponding subscript) being a Poisson subsystem while the other three being Gaussian subsystems, and net G, with all its subpopulations having Gaussian characteristics. The values of $m_j^2\mu^+(1-h)$ and the slope of the partial activity of each subpopulation for the above six nets with four markers with $\mu^+=20$ and 200, are given in Tables 1 and 2, respectively. The slope of the neural activity and the class of the corresponding net are also given in the last two rows of these tables, in each case.

The activity a_{n+1} as a function of the preceding activity a_n for each one of the above six nets with $\mu^+=20$ is given in Fig. 1. In the inset we show a magnification of the origin. The curves are numbered from 1 to 6 corresponding to the six nets. Analogous results for a second group of nets with the same parameters but with relatively large connectivity, $\mu^+=200$, are given in Fig. 2.

The results shown in Table 1 refer to nets with relatively low connectivity. We observe in this table that since the value of the parameter μ^+ is relatively small ($\mu^+=20$), the terms $m_j^2\mu^+(1-h)$ take small values and only in the two large subpopulations a and b they exceed the critical value of unity. Thus, apart from the Poisson P net of class A, for which the slope of the curve of the neural activity at $a_n=0$ is equal to 6, only the nets $P_\alpha G$ with slope 3.2 and $P_b G$ with slope 1.8 (in which the corresponding subpopulation α or b is a Poisson subpopulation) belong to class A. The remaining nets $P_c G$ with slope 0.8, $P_d G$ with slope 0.2 and the Gaussian G net with slope zero belong to class B. The classes of these nets are also seen in the corresponding Fig. 1, where we further observe that for the nets

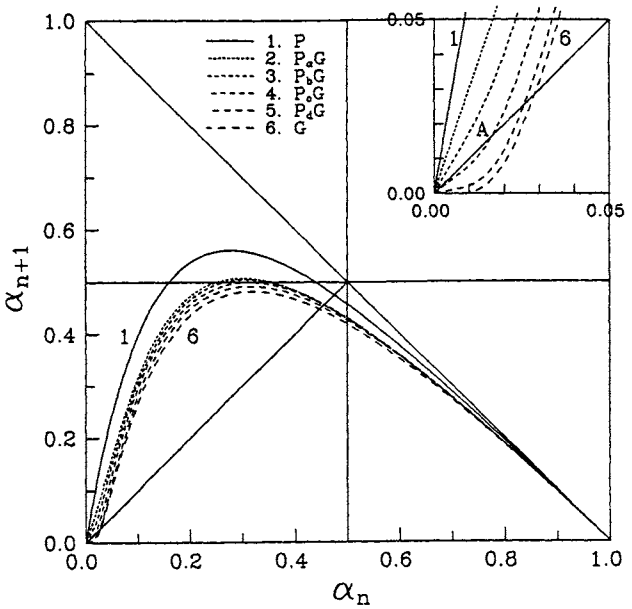

Fig. 1. The total neural activity a_{n+1} vs preceding activity a_n for six isolated nets of four chemical markers, $m_\alpha = 0.4$, $m_b = 0.3$, $m_c = 0.2$, $m_d = 0.1$; with $\vartheta = 1$, $\eta = 1$, $h = 0$, $K^+ = 1$, $r = 1$ and $\mu^+ = 20$. (1) P net, (2) $P_\alpha G$ net, (3) $P_b G$ net, (4) $P_c G$ net, (5) $P_d G$ net and (6) G net. In the upper right corner, a magnified plot of the same curves at the origin is shown.

$P_\alpha G$ and $P_b G$ with the large Poisson subpopulations α and b, respectively, the curves of neural activity have been considerably shifted toward the corresponding curve of the Poisson P net, in spite of the fact that only one Gaussian subpopulation has been substituted by a Poisson one in each case. A noticeable but smaller displacement of the curves toward the corresponding curve of the Poisson P net is also observed for the other nets $P_c G$ and $P_d G$.

In Table 2, for the nets with relatively high connectivity ($\mu^+ = 200$), the values of $m_j^2 \mu^+ (1-h)$ are larger than unity and the corresponding nets with Poisson or hybrid interconnections are of class A. The class of the nets is also seen in Fig. 2, where furthermore we can see the corresponding displacements of the curves of neural activity toward the pure Poisson one. These differences are small since the Gaussian approximation is very good for nets with high connectivity as in the present case.

The time evolution of the neural activity can be seen in Fig. 3, where we plot the activity a_n as a function of time, for the net with $\mu^+ = 20$. Again we used Eq. (5) with the subsequent development with several different initial values. Notice that there are four P curves with $a_{n(t=0)} = 0.015$, 0.2,

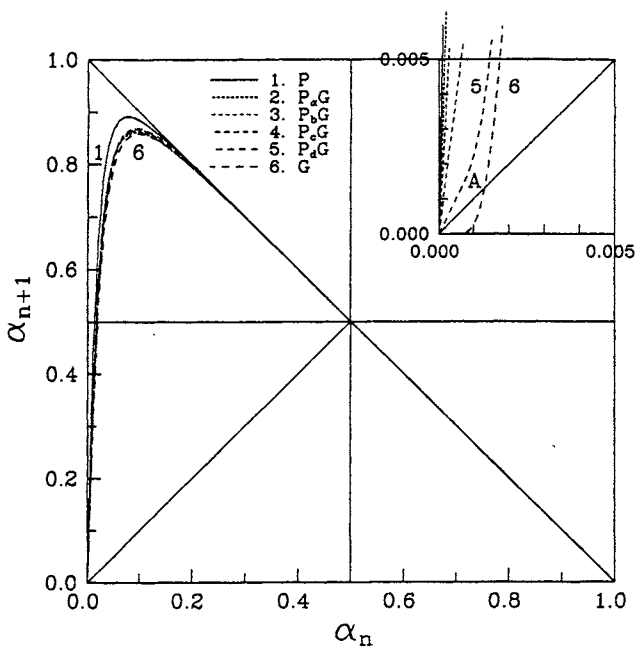

Fig. 2. a_{n+1} vs a_n for six isolated nets of four chemical markers, $m_\alpha = 0.4$, $m_b = 0.3$, $m_c = 0.2$, $m_d = 0.1$; with $\vartheta = 1$, $\eta = 1$, $h = 0$, $K^+ = 1$, $r = 1$ and $\mu^+ = 200$. (1) P net, (2) $P_\alpha G$ net, (3) $P_b G$ net, (4) $P_c G$ net, (5) $P_d G$ net and (6) G net. In the upper right corner, a magnified plot of the same curves at the origin is shown.

0.47 and 0.8. Similarly for the other two cases of $P_c G$ and G nets, as shown in the figure. We observe that for the Poisson net the activities always converge to a constant value, about 0.45, while for the two other nets, Gaussian and hybrid, the long-time activity depends on the initial values. This makes net P to belong to class A, while nets $P_c G$ and G are of class B.

Next, on the basis of the same formalism, we examined non-isolated neural nets, i.e., nets which receive steady or slowly varying external sustained inputs. We used nets of A neurons and two markers, α and b, with $m_\alpha = 0.35$ and $m_b = 0.65$, attached to a cable of afferent fibers which may be axons of $A_o = A$ neurons of another net. The strengths of the synaptic coupling coefficients K_o^+ and K_o^- were chosen arbitrarily to be half of the internal coupling coefficients which is taken to be $K^+ = K^- = 1$. The appropriate values of parameters μ^+ and ϑ are selected for each subsystem in such a way that the hybrid character of the network is clearly shown.

Applying the steady-state condition $a_{n+1} = a_n$, we obtained the phase diagrams and multihysteresis loops shown in Fig. 4, for all three models,

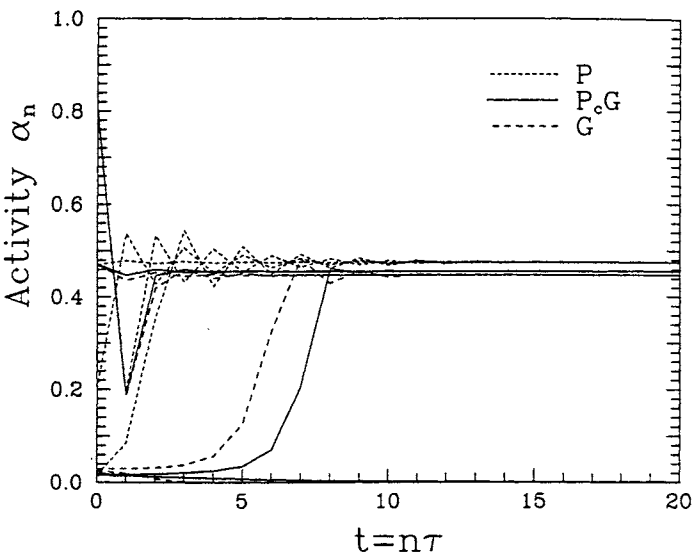

Fig. 3. Time dependence of the total activity a_n for three isolated nets, P, P_cG and G net of four markers, $m_a = 0.4$, $m_b = 0.3$, $m_c = 0.2$, $m_d = 0.1$, with $\vartheta = 1$, $h = 0$, $K^+ = 1$, $r = 1$ and $\mu^+ = 20$. Initial activities: $a_o = 0.015, 0.2, 0.47, 0.8$ for the P net, $a_o = 0.015, 0.017, 0.47, 0.8$ for the P_cG net, and $a_o = 0.025, 0.029, 0.47, 0.8$ for the G net.

Poissonian (P net), Gaussian (G net) and hybrid ($P_\alpha G$ net), for the above nets of two markers α and b, but, for the sake of simplicity, multihysteresis loops are shown only for the hybrid case. Computer simulation results are also depicted in these plots. This diagram combines the data for a purely excitatory input ($h_o = 0$), which is labeled σ^+ and plotted to the right of the origin, with data for a purely inhibitory input ($h_o = 1$), which is labeled σ^- and plotted to the left of the origin. In the non-isolated neural nets, i.e., neural nets receiving external sustained inputs described by the parameter σ, a common property is the appearance of such hysteresis loops. As illustrated here, a slow change of the level of afferent inputs leads to irreversible change in the steady state activity of the net. The parameter a_{ss} is the steady state value of the net activity obtained by requiring that $a_{n+1} = a_n$. The arrows in the diagram indicate the direction of activity change following a fluctuation of activity away from the condition $a_{n+1} = a_n$. The curve is divided into stable and unstable portions (e.g., for the hybrid case, the solid lines indicate the stable portions while the dashed lines the unstable ones). The resulting hysteresis loops have certain reversible portions, linked to each other by irreversible upward transitions

at critical values of $\sigma(\sigma = \sigma_c)$, and downward transitions at other critical values of $\sigma(\sigma = \sigma_o)$. In a network characterized by N markers $2N+1$ portions (or steady states) may appear, from which $N+1$ are the stable ones and N are the unstable ones. Here, in the phase diagrams of Fig. 4 we observe three stable and two unstable steady state portions.

The simple as well as the Multiple hysteresis curves, from a functional point of view, may be considered to represent the basis for short term memory since any input will cause the activity in the neural population to go from the lowest stable into a higher stable state and the activity will remain in this state after the input ceases. Thus, the hysteresis loops may be considered as the basis for short-term memory. Furthermore, since a network may go from a stable state to another due to a change of the external inputs and/or the initial activity, this behavior may be considered as a simple explanation of the sequential thoughts.[13]

In Fig. 5 the neural activity a_{n+1} vs a_n is given for all approximations, Poisson (P net), Gaussian (G net) and hybrid ($P_\alpha G$ net), for nets of two markers α and b, with $\sigma = 0$, as well as computer simulation results. The contribution to the total activity of each marker is also depicted in these plots. For the chosen set of parameters ($\vartheta_\alpha = 2, \mu_\alpha^+ = 33, \vartheta_b = 29, \mu_b^+ = 95$) we obtained two-modal curves[13] of the total neural activity for all cases,

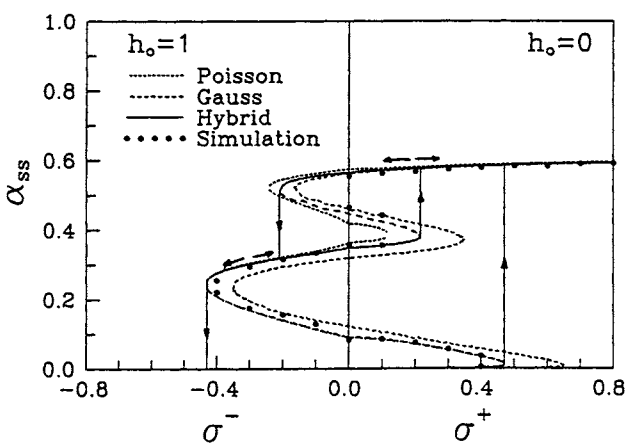

Fig. 4. Phase diagrams and hysteresis curves for three nets (P, G and $P_\alpha G$) with two markers a and b, receiving sustained inputs. The steady-states of activity a_{ss} for these have been plotted against σ. Parameters: $m_\alpha = 0.35$, $m_b = 0.65$; $\mu_\alpha^+ = 56$, $\mu_b^+ = 96$; $h = 0$; $\vartheta_\alpha = 3$, $\vartheta_b = 31$; $r_\alpha = 0, r_b = 1$; $K^+ = 1$, $K_o^+ = K_o^- = 0.5$; $\mu_o^+ = \mu_o^- = 10$. Doted lines are used for the Poisson approximation and dashed lines for the Gaussian one. In the hybrid approximation, solid lines are used for stable steady-states and dashed for unstable states. The solid dots are simulation results.

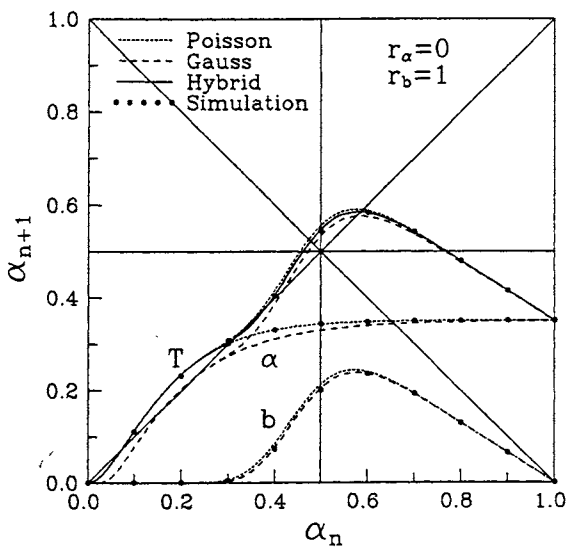

Fig. 5. a_{n+1} vs α_n for three nets (P, G and $P_\alpha G$) with two chemical markers, $m_\alpha = 0.35$ and $m_b = 0.65$, with $\sigma = 0$, $\mu_\alpha^+ = 33$, $\mu_b^+ = 95$, $h = 0$; $\vartheta_\alpha = 2$, $\vartheta_b = 29$; $r_\alpha = 0$, $r_b = 1$; $K^+ = 1$. The curves α and b represent the activities of the corresponding markers, whereas T gives the total activity of the net. The solid lines are used for the hybrid $P_\alpha G$ net, the doted lines for the Poisson P net and the dashed lines for the Gaussian G net. The solid dots are simulation results.

provided that the number of nonzero stable or unstable steady-states are the maximum possible, that is, equal to the number of markers. As a consequence of the large value of ϑ_b, the contribution to the total neural activity of the b marker is restricted to a region beyond the value $a_n \approx 0.3$ of the preceding activity. The differences between the two approximations, Poissonian and Gaussian, in the non saturated parts of b curves are vary small, due mainly to the high connectivity, ($\mu_b^+ = 95$), whereas the corresponding differences in the a curves are large. The simulation results are in very good agreement with the hybrid model.

6. CONCLUSIONS

In this paper we investigated the effect of different neuron connectivities on the dynamical behavior of neural nets with chemical markers. We examined the significance and consequences of assigning different (Poisson or Gaussian) distributions of connectivities on the subnets of the total net, giving now a hybrid character to the overall net. The equation for

the net activity (Eq. (5)) was extended and generalized to include this combination. Our results for hybrid nets, as they are exhibited in Figs. (1) to (5), show a similar general dynamic behavior as in the cases of pure Poisson or Gaussian approximations, i.e., multiple steady states of the neural activity and multiple hysteresis loops in the phase diagrams. We see that when we have only partial substitution of the Poisson approximation with the Gaussian one in the appropriate subsystems, the resulting behavior is in-between these two distributions, as it is shown by the curves in Figs. (4) and (5). Additionally, we find that while a Gaussian net always belongs to class B or C (not guaranteed sustained activity), our new hybrid net may belong to any of the three classes: A (guaranteed sustained activity), B or C. The A class is provided by the newly derived Eq. (17), which gives the slope at the origin ($a_n = 0$) of the neural activity curves (plots of a_{n+1} vs a_n), and has its origin on the Poisson terms of the basic Eq. (5). This behavior was shown by nets $P_\alpha G$ and $P_b G$ of Fig. 1 and by hybrid nets of Fig. 2. We conclude that the distribution laws used to determine the connectivities between neurons in a neural net play an important role in the net behavior.

Finally, as an additional verification, these ideas were analyzed by use of computer simulations. The computational model was designed so that it parallels the developed formalism. For the range of parameters examined we find excellent agreement between these two methods. We note that the analytical method has a probabilistic character and describes an annealed chemical kinetics approach. On the other hand, the simulation results describe a more direct quenched randomness with full specification of the system units. Nevertheless the results of the two methods practically coincide.

APPENDIX

We give here details of the proof of Eq. (17), which gives the slope of the curve a_{n+1} vs a_n as $a_n \to 0$, in the general case of isolated hybrid neural nets with chemical markers; Thus, we take $\partial/\partial a_n(a_{n+1})|_{a_n=0}$ from Eq. (5) for the case of isolated hybrid neural nets ($\sigma = 0$).

For the Poisson subsystems we start from the corresponding Poisson terms of Eq. (5),

$$(a_{n+1})_P = (1 - a_n) \sum_{j=1}^{N_1} m_j P_{Pj}(a_n, m_j, \vartheta_j) \tag{A-1}$$

where

$$P_{Pj}(a_n, m_j, \vartheta_j) = \sum_{I=0}^{I\max,j} \left(1 - \sum_{L=0}^{\eta'_j - 1} P_{L,j}\right) Q_{I,j} \tag{A-2}$$

If we take $\partial/\partial a_n (a_{n+1})_P|_{a_n=0}$ from Eq. (A-1), we find that all terms in the summations over I vanish with the exception of $I=0$ and for this value of I the parameter η' is reduced to $\eta = u[\vartheta_j/K_j^+]$. The final result is

$$\frac{\partial}{\partial a_n}(a_{n+1})_P|_{a_n=0} = \begin{cases} \sum_{j=1}^{N_1} m_j^2 \mu_j^+ (1-h_j) & (\eta_j = 1) \\ 0 & (\eta_j \geqslant 2) \end{cases} \tag{A-3}$$

For the Gaussian subsystems, we first write the Gaussian terms of Eq. (5),

$$(a_{n+1})_G = (1-a_n) \sum_{j=N_1+1}^{N} m_j P_{Gj}(a_n, m_j, \vartheta_j) \tag{A-4}$$

in the form

$$f(x_1, x_2, \ldots, x_N) = (1-a_n) \sum_{j=N_1+1}^{N} m_j P_j(x_j) \tag{A-5}$$

where

$$x_j = \frac{\vartheta_j - \bar{e}_j}{\delta_j} \tag{A-6}$$

and then calculate the partial derivative of f with respect of a_n at $a_n \to 0$, i.e.,

$$\left.\frac{\partial f}{\partial a_n}\right|_{a_n=0} = \frac{\partial}{\partial a_n}\left[(1-a_n) \sum_{j=N_1+1}^{N} m_j P_j(x_j)\right]\Bigg|_{a_n=0} \tag{A-7}$$

from which we have

$$\left.\frac{\partial f}{\partial a_n}\right|_{a_n=0} = \left\{ - \sum_{j=N_1+1}^{N} m_j P_j(x_j) + (1-a_n) \sum_{j=N_1+1}^{N} m_j \frac{\partial P_j(x_j)}{\partial x_j} \frac{dx_j}{da_n} \right\}\Bigg|_{a_n=0} \tag{A-8}$$

Using Eq. (15) with $\sigma = 0$ and applying Leibnitz's theorem we get

$$\frac{\partial P_j(x_j)}{\partial x_j} = -\frac{1}{\sqrt{2\pi}} e^{-x_j^2/2} \tag{A-9}$$

Taking $|K_j^+| = |K_j^-| = K$, $(0 < K < \infty)$ and $\eta_j = \vartheta_j / K_j^+$ it follows from Eq. (A-6) that

$$x_j = \frac{\eta_j - a_n[m_j\mu_j^+(1-h_j) + m_j\mu_j^- h_j]}{\sqrt{a_n[m_j\mu_j^+(1-h_j) + m_j\mu_j^- h_j]}} \tag{A-10}$$

Using $q_j = m_j\mu_j^+(1-h_j)$ and $p_j = m_j\mu_j^- h_j$ we get

$$x_j = \frac{\eta_j + a_n(p_j - q_j)}{\sqrt{a_n(p_j + q_j)}} \tag{A-11}$$

Differentiating this equation with respect to a_n we obtain

$$\frac{dx_j}{da_n} = \frac{-\eta_j + a_n(p_j - q_j)}{2a_n\sqrt{a_n(p_j + q_j)}} \tag{A-12}$$

Taking into account Eqs. (A-9) and (A-12), Eq. (A-8) can be written in the form

$$\left.\frac{\partial f}{\partial a_n}\right|_{a_n=0} = \left\{ -\sum_{j=N_1+1}^{N} m_j P_j(x_j) - \frac{1-a_n}{\sqrt{2\pi}} \times \sum_{j=N_1+1}^{N} m_j e^{-x_j^2/2} \frac{-\eta_j + a_n(p_j - q_j)}{2a_n\sqrt{a_n(p_j + q_j)}} \right\}\Bigg|_{a_n=0} \tag{A-13}$$

from which, after some algebraic manipulation, we get

$$\left.\frac{\partial f}{\partial a_n}\right|_{a_n=0} = \left\{ -\sum_{j=N_1+1}^{N} m_j P_j(x_j) - \frac{1-a_n}{\sqrt{2\pi}} \times \sum_{j=N_1+1}^{N} m_j x_j e^{-x_j^2/2} + \frac{1-a_n}{a_n\sqrt{2\pi}} \sum_{j=N_1+1}^{N} \frac{m_j\eta_j}{\sqrt{a_n(p_j + q_j)}} e^{-x_j^2/2} \right\}\Bigg|_{a_n=0} \tag{A-14}$$

Since as $a_n \to 0$ the $x_j \to \infty$, then it can be easily seen by l'Hospital's rule that

$$\lim_{a_n \to 0} \frac{\partial f(x_j)}{\partial a_n} = 0 \tag{A-15}$$

Thus, the final result for the whole network is the following:

$$\left.\frac{\partial a_{n+1}}{\partial a_n}\right|_{a_n=0} = \begin{cases} \sum_{j=1}^{N_1} m_j^2\mu_j^+(1-h_j) & (\eta_j = 1) \\ 0 & (\eta_j \geqslant 2) \end{cases} \tag{A-16}$$

ACKNOWLEDGMENT

This project was supported by grant No. E5/1943/1993 by the Ministry of Education (Athens), and the Research Committee of TEI Thessaloniki.

REFERENCES

1. W. S. McCulloch and W. Pitts, *Bull. Math. Bio.* **5**:115 (1943).
2. E. R. Caianiello, *J. Theo. Bio.* **2**:204 (1961).
3. H. R. Wilson and J. D. Cowan, *Biophys. J.* **12**:1 (1972).
4. J. S. Griffith, *Biophys. J.* **3**:299 (1963).
5. P. A. Anninos, B. Beek, T. J. Csermely, E. M. Harth, and G. Pertile, *J. Theo. Bio.* **26**:121 (1970); *ibid* **26**:93 (1970).
6. P. A. Anninos and M. Kokkinidis, *J. Theo. Bio.* **109**:95 (1984).
7. P. A. Anninos and R. Elul, *Biophys. J.* **14**:8 (1974).
8. E. Fournou, P. Argyrakis and P. A. Anninos, *Conn. Sci.* **5**:77 (1993).
9. E. Fournou, P. Argyrakis, B. Kargas and P. A. Anninos, *Conn. Sci.* **7**:331 (1995).
10. R. W. Sperry, *J. Comp. Neu.* **79**:33 (1943).
11. R. W. Sperry, *Proceedings of the National Academy of Sciences, USA* **50**:703 (1963).
12. M. C. Prestige and D. J. Willshaw, *Proccedings of the Royal Society, London, B* **90**:77 (1975).
13. A. Adamopoulos and P. A. Anninos, *Conn. Sci.* **1**:393 (1989).